

## Investigation of Contact Resistance Influence on Power Cable Joint Temperature Based on 3-D Coupling Model

**Abstract.** Aiming at the overheating problem of cable joint, a 3-D finite element model of a single-core cable joint considering the coupling of electromagnetic field and temperature field has been built. In order to consider the heat losses generated by contact resistance of cable joint, the equivalent conductivity is calculated. The validity of the model and calculation method is verified by the comparison with analytical values.

**Streszczenie.** Do analizy zagadnienia przegrzania połączenia kablowego zbudowano trójwymiarowy model MES przy uwzględnieniu sprzężenia pola elektromagnetycznego i temperaturowego. W celu określenia strat ciepła wytwarzanego w rezystancji styku połączenia kablowego obliczono konduktywność zastępczą. (Badanie wpływu rezystancji styku połączenia kablowego na temperaturę za pomocą trójwymiarowego modelu sprzężonego).

**Keywords:** Cable joint, Electromagnetic field, Temperature field, Contact resistance.

**Słowa kluczowe:** Połączenie kablowe, Pole elektromagnetyczne, Pole temperaturowe, Rezystancja styku.

### Introduction

Many years of operation experience has shown that due to the existence of contact resistance, poor performance of insulation material, imperfect manufacturing process and bad installation environment, more than 70% of the failures occur at the location of cable joints in power lines. As the weakest link of power cable, overheat of cable joint can lead to open circuit, short circuit, even fire and explosion of power cable and this may result in significant economic losses. [1]. Therefore, temperature is an important indicator to reflect that the operation state of cable joint is good or not.

In previous studies, many scholars focused on the temperature field and ampacity using 2-D model of cable body [2-6]. And there are two methods to calculate the temperature of cable body: one is analytical method based on IEC-60287, another is numerical method [7-9] including boundary element method (BEM), finite element method (FEM), finite volume method (FVM), finite difference method (FDM), etc. However, the 2-D model is not suitable to analyze the temperature property of cable joint, due to the heat transfer in radial direction and in axial direction should be taken into consideration. So this calculation is a complex 3-D problem.

In this paper, a 3-D electromagnetic-thermal coupling analysis model [10-11] of cable joint is established according to the basic theories of electromagnetic field and heat transfer. Based on the given boundary conditions, the electromagnetic field and temperature field distributions are

obtained by using FEM. The effect of contact resistance on temperature of cable joint is taken into consideration in this model by calculating equivalent conductivity at cable joint. The simulation results agree with the analytic results, which can verify the efficiency of the proposed model.

### Methodology

To limit the model complexity, the analysis in this paper is based on the following basic assumptions:

- Due to the frequency is equal to 50 Hz, the displacement current can be neglected;
- Only the steady-state conditions are studied;

Based on the above assumptions and Maxwell equations, the magnetic vector potential equation can be described. [12]

$$(1) \quad (\nabla \cdot \frac{1}{\mu} \nabla) A = -J_s + j\omega\sigma A$$

where:  $\mu$  – permeability,  $A$  – magnetic vector potential,  $\sigma$  – electrical conductivity,  $J_s$  – current density,  $\omega$  – angular frequency.

The electrical conductivity of copper can be expressed by the following equation. [13]

$$(2) \quad \sigma = \frac{\sigma_{20}}{1 + \alpha(T - 20)}$$

where:  $\sigma_{20}$  – electrical conductivity at 293.15 K,  $\alpha$  – temperature coefficient,  $T$  – temperature.

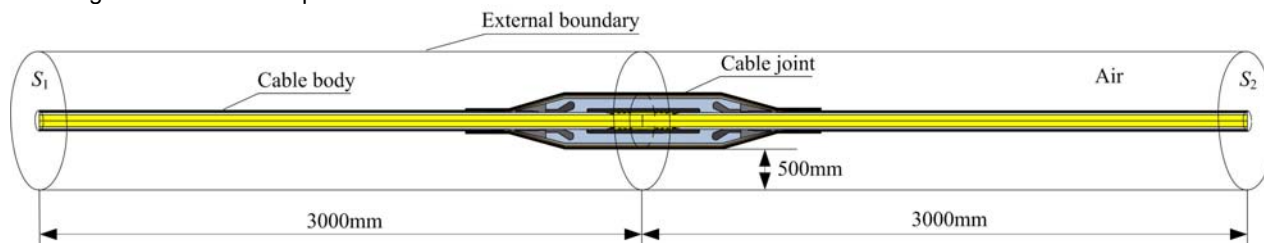


Fig. 1. The closed region model of cable joint.

The boundary conditions of the model (as shown in Fig. 1) for electromagnetic analysis are given as follows:

- The magnetic vector potential  $A$  at the external boundary of air domain is equal to zero;
- A sinusoidal alternating current is given at the cross-section of cable conductor;
- The boundary conditions at  $S_1$  and  $S_2$  are magnetic insulation.

The associated steady-state heat conduction equation for 3-D cable joint can be described by the following equation. [14]

$$(3) \quad \nabla \cdot (\lambda \nabla T) + Q_v = 0$$

where:  $\lambda$  – thermal conductivity,  $Q_v$  – heat source per unit volume.

The boundary conditions of the model for thermal analysis are given as follows:

a) At the outer surface of cable, the natural convection boundary condition and the heat radiation boundary condition are given;

b) The boundary conditions at  $S_1$  and  $S_2$  are thermal insulation.

Due to the existence of contact resistance, the current lines will shrink when the current flows through the contact surface, which can lead to the increase of current density, electromagnetic loss and temperature of connections. In order to consider the influence of contact resistance, the connection tube and conductor are simplified into a whole with an equivalent conductivity (as shown in Fig. 2).

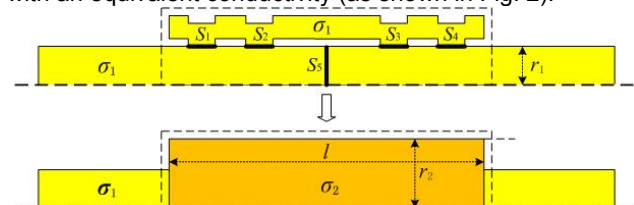


Fig. 2. Structure and equivalent simulation model of cable conductor joint

The equivalent conductivity can be expressed as:

$$(4) \quad \sigma_2 = \frac{\sigma_1}{k} \cdot \left( \frac{r_1}{r_2} \right)^2$$

where:  $\sigma_1$  – electrical conductivity of cable conductor,  $\sigma_2$  – equivalent electrical conductivity,  $r_1$  – radius of cable conductor,  $\sigma_2$  – equivalent electrical conductivity;  $r_2$  – outer radius of the connection tube,  $k$  – ratio.

In the actual engineering, the value of  $k$  is usually greater than 1 due to the existence of contact resistance which is caused by irregular construction of cable joint.

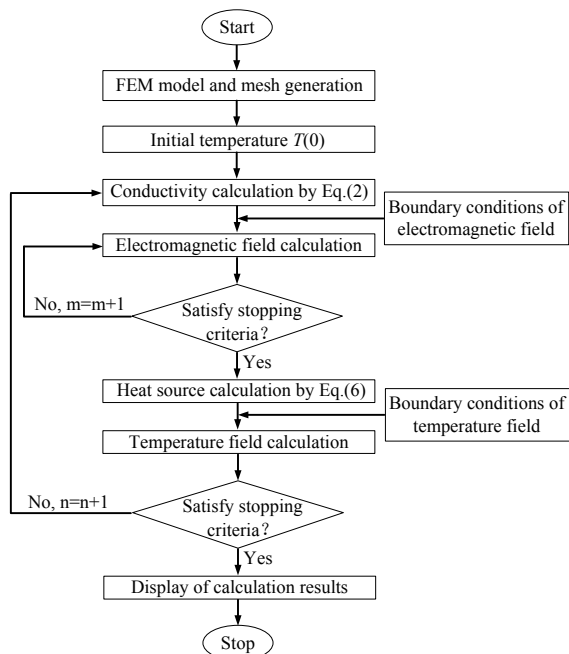


Fig. 3. Flow chart of electromagnetic-thermal coupling model

The heat source of cable mainly results from Joule losses caused by the conductor current. The  $Q_v$  can be calculated as follows: [15]

$$(5) \quad \mathbf{J} = \nabla \times \frac{1}{\mu} \nabla \times \mathbf{A}$$

$$(6) \quad Q_v = \frac{1}{\sigma} |\mathbf{J}|^2$$

A double iterative algorithm is used to calculate the electromagnetic-thermal coupling model and the calculation flow chart is shown in Fig. 3.

### Example Calculation and Validation

To calculate the 3-D electromagnetic-thermal coupling fields of the cable joint, the type of 8.7/15 kV YJV 1×400 XLPE cable is taken for an example in this part. The cable ratings are given in Table 1.

Table 1. Basic parameters of simulated cable

Physical quantities	Value
Conductor diameter (mm)	23.8
Insulation thickness (mm)	4.5
Shielding layer thickness (mm)	0.5
Sheath thickness (mm)	2.5
External diameter of Cable (mm)	41
Cable size (mm <sup>2</sup> )	400
Rated frequency (Hz)	50

When  $J_s$  is 645A, ambient temperature is 298.15 K and  $k$  is 5, the distributions of  $Q_v$  and  $T$  are shown in Fig. 4 and Fig. 5.

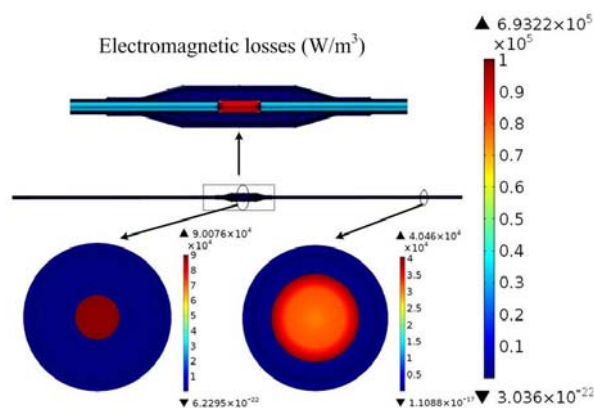


Fig.4. 3-D distribution of  $Q_v$  of cable joint.

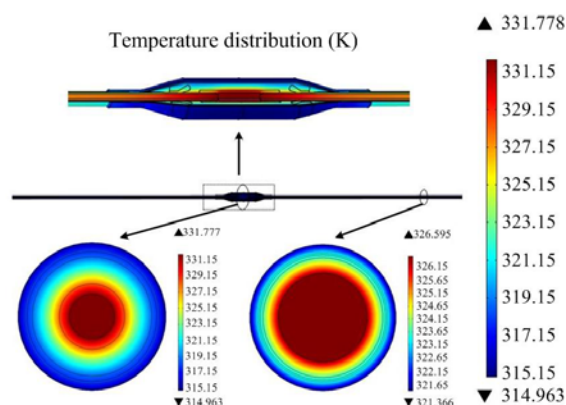


Fig.5. 3-D distribution of  $T$  of cable joint.

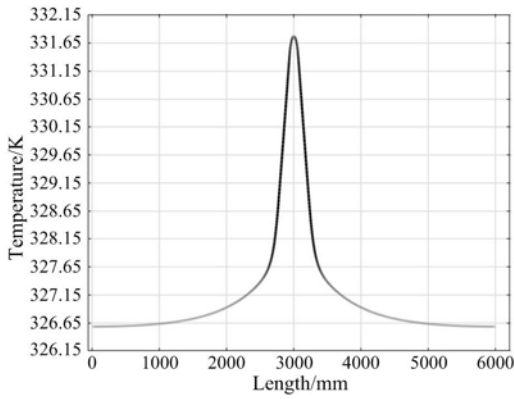


Fig. 6. Axial temperature field distribution curve of cable core

Fig. 4 shows that the electromagnetic losses are mainly distributed in the region near the conductor surface. Fig. 5 shows that the highest temperature of cable joint is 5.18 K higher than that of cable body due to its greater electromagnetic losses. It is observed in Fig. 6 that the conductor temperature of the cable body (2 meters from the center of cable joint) is little affected by the cable joint temperature, which means that the heat transfer in axial direction is limited to the region within 2 meters of cable joint.

In order to verify the accuracy of the proposed method in this paper, the calculated results of  $|H|_{\max}$  and  $Q_v$  of cable body based are compared with the analytical results, as shown in Table 2. The analytical results are calculated based on the IEC-60287 standard [16-17].

Table 2. Result comparison between two different methods

Parameters	Analytical method	Proposed method	Relative error/%
$ H _{\max}$ (A/m)	1.1435e4	1.1429e4	0.052
$Q_v$ (W/m <sup>3</sup> )	3.3844e4	3.377e4	0.22

It can be indicated that the relative errors between the calculated values of  $|H|_{\max}$  and  $Q_v$  based on the analytical method and that based on the electromagnetic-thermal FEM are within 5 %.

### Discussion

As one of main factors influencing the thermal property of cable joint, the contact resistance at conductor joint directly affects the electromagnetic losses. The greater the contact resistance will result in more heat generation and higher temperature rise. Conversely, the less the contact resistance will result in less heat generation and lower temperature rise. With other conditions remaining unchanged, the axial temperature field distribution curves of cable core with different values of  $k$  are shown in Fig. 7 and Fig. 8 shows the highest temperature distribution curves of cable body and cable joint with different values of  $k$ .

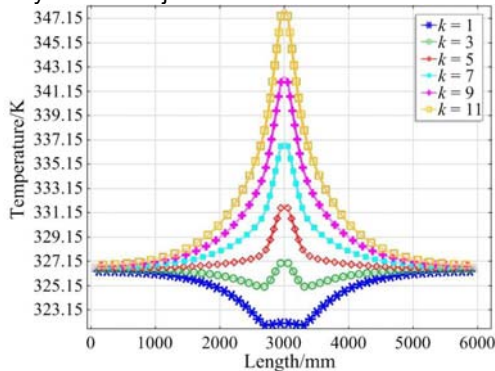


Fig. 7. Axial temperature field distribution curves with  $k$

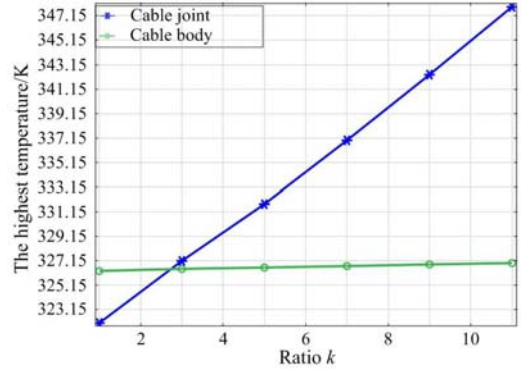


Fig. 8. The highest temperature distribution curves of cable with  $k$

It can be noted that the temperature of cable joint increases with the increase of  $k$  and the increase rate of the highest temperature also has a slight growth. For example, when the value of  $k$  changes from 1 to 3, the highest temperature of joint conductor has an increase of 5.09 K from 322.05 K to 327.14 K, whereas when the value of  $k$  changes from 9 to 11, the highest temperature of joint conductor has an increase of 5.56 K from 342.33 K to 347.89 K. This is caused by the combined effects of heat source, equivalent conductivity and temperature shown in equation (2) and equation (6). The contact resistance at cable joint has a negligible effect on the temperature of cable body which is 2.5 meters from the center of cable joint, and this is because the heat transfer in axial direction of cable body can be ignored.

Fig. 7 and Fig. 8 also show that when the value of  $k$  is less than 2.7, the conductor temperature of cable body is higher than that of cable joint because of the stronger heat dissipation at cable joint, though the heat source at cable joint is greater. However, when the value of  $k$  is greater than 2.7, the conductor temperature of cable joint is higher than that of cable body due to the dominant role of heat generation compared with heat dissipation of cable joint.

### Conclusion

The electromagnetic-thermal coupling analysis model of the cable joint is established based on the 3-D finite element method (FEM), the distributions of electromagnetic-thermal coupling fields are obtained by a double iterative algorithm and the calculation method is proved to be correct by comparing with analytical method. The results show that the existence of the contact resistance can result in increasing the electromagnetic loss and temperature rise of cable joint, and the heat transfer in axial direction is more obvious only within 2 meters of the cable joint center. The contact resistance significantly affects the temperature of the cable joint and there is a positive correlation between them. Considering the cable ampacity from a global viewpoint, the ratio of the equivalent resistance at the cable joint to the resistance at cable body should be less than 2.7.

### ACKNOWLEDGMENT

This work was supported by the East Inner Mongolia Electric Power Company Limited, the National Natural Science Foundation of China (Grant No. 51477013), the Major State Basic Research Development Program of China (973 Program, No. 2011CB209401) and the Fundamental Research Funds for Central Universities (No. CDJZR14155501).

**Authors:**

Luo Hanwu, Liu Haibo and Kang Kai are with East Inner Mongolia Electric Power Company Limited, Hohhot 010020, China.  
Cheng Peng, Yang Fan and Yang Qi are with the State Key Laboratory of Power Transmission Equipment & System Security and New Technology, School of Electrical Engineering, Chongqing University, Chongqing 400044 China (e-mail: [chengpeng19870825@163.com](mailto:chengpeng19870825@163.com)).

## REFERENCES

- [1] Yomna O, et al, Thermal modeling of medium voltage cable terminations under square pulses, IEEE Trans. Dielectr. Electr. Insul., vol. 21, no. 3, pp. 932-939, Jun. 2014.
- [2] Rasmus Olsen, et al, Modelling of dynamic transmission cable temperature considering soil-specific heat, thermal resistivity, and precipitation, IEEE Trans. Power Del., vol. 28, no. 3, pp. 1909-1917, Jul. 2013.
- [3] Ali Sedaghat, et al, Thermal analysis of power cables in free air: Evaluation and improvement of the IEC standard ampacity calculation, IEEE Trans. Power Del., vol. 29, no. 5, pp. 2306-2314, Oct. 2014
- [4] James A, et al, Rating of cables in unfilled surface troughs, IEEE Trans. Power Del., vol. 27, no. 2, pp. 993-1001, Apr. 2012.
- [5] Merkebu Z, et al, Comparison of air-gap thermal models for MV power cables inside unfilled conduit, IEEE Trans. Power Del., vol. 27, no. 3, pp. 1662-1669, Jul. 2012.
- [6] George J, et al, Ampacity calculation for cables in shallow troughs, IEEE Trans. Power Del., vol. 25, no. 4, pp. 2064-2072, Oct. 2010.
- [7] G. Gela, J. J. Dai, Calculation of thermal fields of underground cables using the boundary element method, IEEE Trans. Power Del., vol. 5, no. 3, pp. 1341-1347, Oct. 1988.
- [8] G.J. Anders, et al, New approach to ampacity evaluation of cables in ducts using finite element technique, IEEE Trans. Power Del., vol. 2, no. 4, pp. 969-975, Oct. 1987.
- [9] Ngockhoa Nguyen, et al, New approach of thermal field and ampacity of underground cables using adaptive hp-FEM, in Proc. IEEE PES 2010 General Meeting, pp. 1-5, April 19-22, New Orleans, LA, USA.
- [10] M'hemed Racheq and Soraya Nati Larbi, Magnetic eddy-current and thermal coupled models for the finite-element behavior analysis of underground power cables, IEEE Trans. Magn., vol. 44, no. 12, pp. 4739-4746, Dec. 2008.
- [11] Li Ling, et al, Thermal field calculation and influencing parameters analysis of gas insulated busbars, Transactions of China Electrotechnical Society, vol. 27, no. 9, pp. 264-270, Sep. 2012.
- [12] S.W.Kim, et al, Coupled Finite-element-Analytic Technique for Prediction of Temperature Rise in Power Apparatus, IEEE Trans. Magn., vol. 38, no. 2, pp. 921-924, Mar. 2002.
- [13] Juan Carlos, et al, Influence of different types of magnetic shields on the thermal behavior and ampacity of underground power cables," IEEE Trans. Power Del., vol. 26, no. 4, pp. 2659-2667, Oct. 2011.
- [14] Y. Shiming, T. Wenquan, Heat transfer, Higher Education Press, Beijing, China, 2006 (In Chinese).
- [15] Lin Shuyi, Xu Zhihong, Simulation and analysis on the three-dimensional temperature field of AC solenoid valves, (in Chinese) Proce. CSEE, vol. 32, no. 36, pp. 156-164, Dec. 2012.
- [16] Electric cables – Calculation of the current rating: Current rating equations (100% load factor) and calculation of losses – general, IEC Std. 60287-1-1, 2<sup>nd</sup> ed., 2006.
- [17] Electric cables – Calculation of the current rating: Current rating equations (100% load factor) and calculation of losses – thermal resistance, IEC Std. 60287-2-1, 2<sup>nd</sup> ed., 2006.